online data

Numerous transcriptional alterations in liver persist after short-term enzyme-replacement therapy in a murine model of mucopolysaccharidosis type VII

Josh C. WOLOSZYNEK*, Marie ROBERTS*, Trey COLEMAN*, Carole VOGLER†, William SLY‡, Clay F. SEMENKOVICH*§ and Mark S. SANDS*‖[1]

*Department of Medicine, Washington University School of Medicine, St. Louis, MO 63110, U.S.A., †Department of Pathology, Saint Louis University School of Medicine, St. Louis, MO 63104, U.S.A., ‡The Edward A. Doisy Department of Biochemistry and Molecular Biology, Saint Louis University School of Medicine, St. Louis, MO 63104, U.S.A., §Department of Cell Biology and Physiology, Washington University School of Medicine, St. Louis, MO 63110, U.S.A., and ‖Department of Genetics, Washington University School of Medicine, St. Louis, MO 63110, U.S.A.

The lysosomal storage disease MPS VII (mucopolysaccharidosis type VII) is caused by a deficiency in β-glucuronidase activity, and results in the accumulation of partially degraded glycosaminoglycans in many cell types. Although MPS VII is a simple monogenetic disorder, the clinical presentation is complex and incompletely understood. ERT (enzyme replacement therapy) is relatively effective at improving the clinical course of the disease; however, some pathologies persist. In order to clarify the molecular events contributing to the disease phenotype and how ERT might impact upon them, we analysed liver tissue from untreated and treated MPS VII mice at both 2 and 5 months of age using biochemical assays and microarray analysis. Overall, as the disease progresses, more genes have altered expression and, at either age, numerous transcriptional changes in multiple pathways appear to be refractory to therapy. With respect to the primary site of disease, both transcriptional and post-transcriptional mechanisms are involved in the regulation of lysosomal enzymes and other lysosome-associated proteins. Many of the changes observed in both lysosome-associated mRNAs and proteins are normalized by enzyme replacement. In addition, gene expression changes in seemingly unrelated pathways may account for the complex metabolic phenotype of the MPS VII mouse. In particular, β-glucuronidase deficiency appears to induce physiological malnutrition in MPS VII mice. Malnutrition may account for the pronounced adipose storage deficiency observed in this animal. Studying the molecular response to lysosomal storage, especially those changes recalcitrant to therapy, has revealed additional targets that may improve the efficacy of existing therapies.

Key words: enzyme replacement, β-glucuronidase, lysosomal storage, mucopolysaccharidosis, Sly syndrome.

INTRODUCTION

The lysosome has many functions, ranging from degrading macromolecules and organelles to processing peptides for antigen presentation [1]. In a group of inherited metabolic disorders referred to as LSDs (lysosomal storage diseases), the loss of an acid hydrolase results in the accumulation of partially degraded substrates in the lysosomes of many cell types [2]. The mucopolysaccharidoses are a subset of lysosomal enzyme deficiencies that result in the inability to completely degrade GAGs (glycosaminoglycans). MPS VII (mucopolysaccharidosis type VII) is caused by a deficiency in GUSB (β-glucuronidase) activity [3]. MPS VII is a progressive disease resulting in the accumulation of heparan sulphate, dermatan sulphate and chondroitin sulphate in many cells of the body. Patients with MPS VII have a broad spectrum of clinical signs, including hearing and visual impairment, mental retardation, skeletal dysmorphism and shortened lifespan [4]. One murine model of MPS VII has a single base-pair deletion in exon 10 of the *GUSB* gene, is deficient in GUSB enzyme activity, and shares most of the clinical signs of the human disease [5–7].

Although MPS VII is a simple monogenetic disease, it results in a complex biochemical and clinical phenotype. The underlying molecular events that occur as the disease progresses are incompletely understood. For example, as GAGs accumulate in distended lysosomes, the levels of certain other lysosomal enzymes increase [8]. Paradoxically, however, substrates other than GAGs also accumulate in affected cells [9]. It is unlikely that this secondary accumulation is due to deficiencies in other lysosomal enzymes, but rather suggests that there may be a global lysosome dysfunction associated with GUSB deficiency.

In addition to the complex biochemical phenotype, there are also secondary clinical phenotypes linked to GUSB deficiency. For example, the MPS VII mouse was originally identified as the ASD (adipose storage deficiency) mouse due to the paucity of abdominal fat stores [10]. Very little is known as to how GUSB deficiency results in the adipose-deficient phenotype. It has also been shown that genetic heterogeneity can affect the clinical presentation, but it is unclear what role modifying genes play in the primary and secondary phenotypes [11].

The MPS VII mouse has been used extensively as a model system for studying methods designed to treat LSDs. These include BMT (bone marrow transplantation), ERT (enzyme replacement therapy), gene therapy and combination therapy [12,13]. These therapies have been effective in alleviating many of the clinical signs of this disease. However, not all the clinical phenotypes are completely corrected. For example, the skeletal dysplasia is not completely rescued by any of the treatments, even if the

Abbreviations used: BMT, bone marrow transplantation; (CI-)MPR, (cation-independent) mannose-6-phosphate receptor; ERT, enzyme replacement therapy; GAG, glycosaminoglycan; GUSB, β-glucuronidase; HRP, horseradish peroxidase; IGFBP, insulin-like-growth-factor-binding protein; LAMP-1, lysosome-associated membrane protein 1; LSD, lysosomal storage disease; MPS VII, mucopolysaccharidosis type VII; NEFA, non-esterified fatty acid; RT-PCR, reverse transcriptase-PCR; TBS, Tris-buffered saline; TGN, *trans*-Golgi network.

[1] To whom correspondence should be addressed (e-mail msands@im.wustl.edu).

therapy is initiated at birth when lysosomal storage is minimal [13–15]. Although normalized early in life by BMT, hearing defects become progressively worse as treated mutants age [16]. Even though retinal function is improved following BMT, some histopathological lesions persist in the eye [17]. Finally, even with persistent high-level expression of GUSB from a gene therapy vector, lifespan and auditory function are not completely normalized [15]. Understanding why these approaches only partially correct the disease phenotype may uncover additional therapeutic targets.

The complexity of the biochemical and clinical phenotypes and the inability to correct these defects completely led us to perform comprehensive biochemical and molecular analyses of untreated and treated MPS VII mice. Using standard biochemical assays and DNA microarray analysis, we have determined some of the primary and secondary alterations in the livers of MPS VII mice at both 2 and 5 months of age. We have also determined how ERT affects these changes. Our data support early intervention. In addition, previously unknown alterations in other metabolic pathways were discovered. Importantly, we identified numerous transcriptional alterations resistant to ERT. This information will enhance our understanding of the disease process, and may provide additional targets for effective therapy.

EXPERIMENTAL

MPS VII mice and ERT

The MPS VII colony is maintained as a pedigree colony through strict brother–sister matings at Washington University by M. S. Sands. Wild-type (+/+) and mutant MPS VII (B6.C-*H-2*^{bml}/ByBir-*gus*$^{mps/mps}$) mice were identified by a combination of biochemical and PCR genotyping [18]. All mice were fed on high-fat (9 %) PicoLab Mouse Chow 20 #5058 ad lib. (LabDiet/PMI Nutrition International, St Louis, MO, U.S.A.). All animal experiments were approved by the IACUC (Institutional Animal Care and Use Committee) at Washington University.

Two separate sets of male wild-type MPS VII mice and MPS VII mice that received ERT were analysed at 2 and 5 months of age. For the 2-month time point, three 7-week-old homozygous mutant MPS VII males received the first of three weekly intravenous injections of GUSB, and will hereafter be referred to as 2moERT mice. The 2moERT mice were then killed 48 h after the last injection. For the 5-month time point, three 21–22-week-old mutant MPS VII males received the first of three weekly intravenous injections of GUSB, and will hereafter be referred to as 5moERT mice. The 5moERT mice were also killed 48 h after the last injection. The 2moERT mice received 19 000 units of a 1:1 mixture of highly phosphorylated (produced in mammalian cells) and non-phosphorylated (produced in baculovirus) GUSB in 200 μl of dilution buffer [150 mM NaCl/10 mM Tris/HCl (pH 7.5)/1 mM β-glycerophosphate] [19]. The 5moERT mice received 25 000 units of GUSB containing approx. 70 % phosphorylated and 30 % non-phosphorylated enzyme, as determined by differential uptake in fibroblasts or macrophages, in 150 μl of dilution buffer [20].

Histopathology

Portions of liver were individually immersed in 2 % glutaraldehyde/4 % paraformaldehyde (w/v) in PBS, and embedded in Spurr's resin. Sections of tissue (0.5 μm in thickness) were stained with Toluidine Blue and evaluated for lysosomal storage by light microscopy.

Oligonucleotide microarray analysis

Three mice each from the wild-type (+/+), MPS VII (*gus*^{mps}/*gus*^{mps}) and ERT-treated MPS VII groups were used for isolating liver tissue. RNA was purified according to the manufacturer's specification from liver tissue using TRIzol® reagent (Invitrogen, Carlsbad, CA, U.S.A.). The integrity of the RNA was confirmed by formaldehyde–agarose gel electrophoresis. To control for animal-to-animal variation, equal amounts of RNA from the three mice in each group were pooled. Double-stranded cDNA was prepared from 10 μg of pooled RNA using an oligo(dT) primer containing the T7 promoter. *In vitro* transcription utilizing the Bioarray High Yield kit (Enzo, Farmingdale, NY, U.S.A.) was used to create biotinylated cRNA probes. After fragmentation, the cRNA was hybridized to the MU74Av2 GeneChip (Affymetrix, Santa Clara, CA, U.S.A.). Signals from the hybridized cRNA were quantified, and Microarray Suite 5.0 (Affymetrix) was used to make comparisons between GeneChips. Microarray data were only included in our analyses if the mRNA was determined to be present at a P value of $\leqslant 0.04$ with a signal value $\geqslant 100$ (after comparison) in both wild-type mice and the experimental group (either MPS VII or MPS VII ERT-treated mice). BLAST analysis (National Center for Biotechnology Information) was used to identify genes not annotated by Affymetrix, and includes GenBank® identities used to derive probes.

Quantitative RT (reverse transcriptase)-PCR analysis

For most of the genes analysed by quantitative RT-PCR, 10 μg of pooled total RNA from each group was used to prepare cDNA. Owing to the low abundance of mRNA for the CI-MPR (cation-independent mannose-6-phosphate receptor), as well as the lysosomal enzymes β-hexosaminidase, α-galactosidase and α-*N*-acetylglucosaminidase, 1 μg of polyadenylated [poly(A)$^+$] RNA was used to prepare cDNA. Quantitative RT-PCR measuring increasing fluorescence of the SYBR Green dye in real time utilizing the TaqMan 5700 sequence detection system (Applied Biosystems, Foster City, CA, U.S.A.) was performed. Three or four serial dilutions of cDNA were used to create a standard curve from cycle thresholds allowing for comparisons between samples. A standard curve of cycle thresholds for glyceraldehyde-3-phosphate dehydrogenase was used to normalize between the groups. All PCR reactions were performed in duplicate. Sequences for the primer sets are available from the authors upon request.

Biochemistry

Portions of liver from all the mice used for the microarray analysis were flash-frozen in liquid nitrogen and stored at -80 °C. The samples were homogenized in buffer containing 150 mM NaCl, 10 mM Tris/HCl, pH 7.5, 1 mM dithiothreitol and 0.2 % (v/v) Triton X-100, and assayed for the amount of total protein using the Coomassie Blue dye-binding assay (Bio-Rad, Hercules, CA, U.S.A.). The activities of the lysosomal enzymes GUSB, α-galactosidase, β-hexosaminidase and α-*N*-acetylglucosaminidase were determined using the fluorescent substrates 4-methylumbelliferyl β-D-glucuronide, 4-methylumbelliferyl α-D-galactoside, 4-methylumbelliferyl β-D-glucosaminide and 4-methylumbelliferyl *N*-acetyl-α-D-glucosaminide (Sigma, St Louis, MO, U.S.A.) respectively, as described previously [14]. The results are reported as specific activities (nmol of 4-methylumbelliferyl released/h per mg of total protein). The activity of acid sphingomyelinase was assayed with the Amplex Red Sphingomyelinase Assay Kit (Molecular Probes, Eugene, OR, U.S.A.) [21]. The specific activity for acid sphingomyelinase is reported as arbitrary fluorescence units/h per mg of total protein.

Western blot analysis

Protein homogenates were prepared from the livers of the 9-week-old wild-type, MPS VII and ERT-treated MPS VII mice. Liver tissue was homogenized (1 μg per 25 μl of buffer) in ice-cold RIPA buffer [150 mM NaCl/50 mM Tris/HCl (pH 8.0)/1 mM EDTA/0.5 % sodium deoxycholate/0.1 % (w/v) SDS/0.1 % Nonidet P40/0.01 % sodium azide/1 % protease inhibitor cocktail (Sigma)], incubated for 10 min on ice, and centrifuged at 16 000 ***g*** in a microcentrifuge at 4 °C. Supernatant was removed and stored at − 80 °C. Supernatants were assayed for total protein using the Coomassie Blue dye-binding assay. Samples containing equal amounts of protein were prepared, denatured by boiling for 10 min in RIPA buffer, and loaded on to a 6 % (w/v) acrylamide gel with a 5 % stacking gel. Protein was transferred overnight to nitrocellulose with the Mini Trans-Blot Transfer Cell (Bio-Rad). Filters were incubated in blocking buffer [5 % non-fat powdered milk/0.01 % (v/v) Tween 20/0.01 % sodium azide in PBS] for 1 h at room temperature (≈ 25 °C). The filter was incubated overnight with a rabbit anti-(mannose receptor) antibody (kindly given by Dr P. Stahl at Washington University) diluted 1:20 000 in blocking buffer, then washed three times for 10 min with 1 × TBS (Tris-buffered saline)/0.1 % Tween 20. Goat anti-rabbit HRP (horseradish peroxidase) secondary antibody (Sigma) diluted 1:20 000 in 1 × TBS/0.1 % Tween 20 was added and incubated for 1 h at room temperature, then washed for 10 min with 1 × TBS/0.1 % Tween 20, and subsequently washed for a further 10 min with 2 × TBS. Equal parts of 0.25 mM luminol (Sigma) and 0.33 mM *p*-coumaric acid (Sigma) in 0.1 M Tris/HCl, pH 8.5, and 0.008 % hydrogen peroxide in 0.1 M Tris/HCl, pH 8.5, were added to the filter for 1 min and exposed to Kodak (Rochester, NY, U.S.A.) film. A separate filter was incubated overnight with a rat anti-mouse LAMP-1 (lysosome-associated membrane protein 1) antibody (Pharmingen, San Diego, CA, U.S.A.) diluted 1:600 in blocking buffer, then probed as described above using a goat anti-rat secondary antibody (Amersham Biosciences, Uppsala, Sweden) diluted 1:6000. Another filter was incubated overnight with a rabbit anti-bovine CI-MPR antibody (kindly given by Dr. S. Kornfeld at Washington University) diluted 1:750 in blocking buffer, then probed as described above using a donkey anti-rabbit secondary antibody (Amersham) diluted 1:2000. Confirmation that equal amounts of protein homogenates were loaded on to the gels was determined by re-probing two of the filters (LAMP-1 and CI-MPR) with an anti-β-actin antibody (Sigma) diluted 1:5000 in blocking buffer. A second gel was used for controlling the levels of protein homogenates used for detecting the mannose receptor. The β-actin antibody was detected by incubation with sheep anti-mouse HRP (Amersham) diluted 1:10 000 in 1 × TBS/0.1 % Tween 20, and exposed as described above. Changes in protein levels were measured semi-quantitatively using the densitometry function of the IS-1000 digital imaging system (Alpha Innotech, San Leandro, CA, U.S.A.) to measure films exposed for different lengths of time.

Plasma chemistries

For the plasma chemistries, wild-type mice, mice heterozygous for MPS VII and homozygous MPS VII mice were fasted for 4–6 h, and then bled from the saphenous vein with heparinized capillary tubes (Fisher, Hampton, NH, U.S.A.). The whole blood was collected in EDTA-containing Microtainer collection tubes (Becton Dickson, Franklin Lakes, NJ, U.S.A.). Plasma was collected by centrifugation by spinning at 2940 ***g*** for 5 min. Total cholesterol (Sigma), triacylglycerols (Sigma) and non-esterified fatty acids (Wako, Richmond, VA, U.S.A.) were analysed in duplicate as described previously [22].

Statistical significance was determined using the two-tailed Student's *t* test assuming equal variance.

RESULTS

Reduction of liver lysosomal storage by ERT

MPS VII mice are known to accumulate small amounts of partially degraded GAGs in cells of the reticuloendothelial system (Kupffer cells) of the liver as early as 15.5 days gestation [23]. By weaning, storage is consistently seen in Kupffer cells, endothelial cells and hepatocytes of the liver. The accumulation of storage is progressive as the animals age.

In order to address the progressive nature of the disease and to determine the effect of ERT on lysosomal storage as the mice age, untreated and treated MPS VII mice at either 2 or 5 months of age were analysed and compared with age-matched wild-type mice. At both time points, untreated MPS VII mice have pronounced lysosomal storage in the liver. However, MPS VII mice at either age that are given a regimen of three injections of recombinant GUSB spaced 1 week apart have substantially reduced storage (Figure 1A). The levels of GUSB activity in the ERT-treated MPS VII mice were 6.1 % and 17.9 % those of normal levels at the 2- and 5-month time points respectively (Figure 1B). Intravenously administered recombinant GUSB, both phosphorylated and non-phosphorylated, has previously been shown to have a half-life of between 36 and 50 h [19,24]. Based on the input dose, the $t_{1/2}$ of the enzyme, and the levels of GUSB at the time of killing (48 h after the final injection), the levels of GUSB throughout the treatment regimen probably never fell below 1–3 % of normal liver levels. Previous studies have shown that as little as 1–2 % of normal enzyme levels are sufficient to virtually eliminate storage [25,26]. In addition, after elimination of lysosomal storage by ERT, the reappearance of identifiable lysosomal storage in the liver was delayed for approx. 4 weeks [27]. Therefore we believe the enzyme regimen used in the current study was efficacious throughout the treatment period, and thus liver tissue derived from these mice could serve as an example of a tissue that was responsive to therapy.

Global changes in mRNA expression

As mentioned previously, the accumulation of partially degraded GAGs begins shortly before birth and gradually increases with age. The clinical course of the disease also becomes increasingly complex. We used microarrays to examine gene expression on an organ-wide scale. Portions of liver from the same mice described in Figure 1 were used as the source of RNA from which cDNA was prepared. Levels of mRNA in MPS VII animals that were both detectable and whose expression changed by 2-fold or greater, as compared with age-matched wild-type mice, were analysed further.

We noticed two general trends. First, as the untreated MPS VII animals age from 2 to 5 months, the number of genes with expression changes of 2-fold or greater increases from 23 to 76 (Figures 2A and 2B). Secondly, of the genes with 2-fold or greater changes in expression, a similar percentage of them return to baseline (i.e. less than a 2-fold change) following ERT at both 2 months and 5 months. At 2 months of age and with an average of 6.1 ± 2.9 % of the mean wild-type enzyme activity, the expression levels of 52 % of the altered genes returned to wild-type levels. Similarly, at 5 months of age and with an average of 17.9 ± 2.3 % of the mean wild-type enzyme activity, 51 % of the genes with altered expression returned to the baseline (Figure 2B). The number of genes with altered expression after ERT was approx. 3-fold

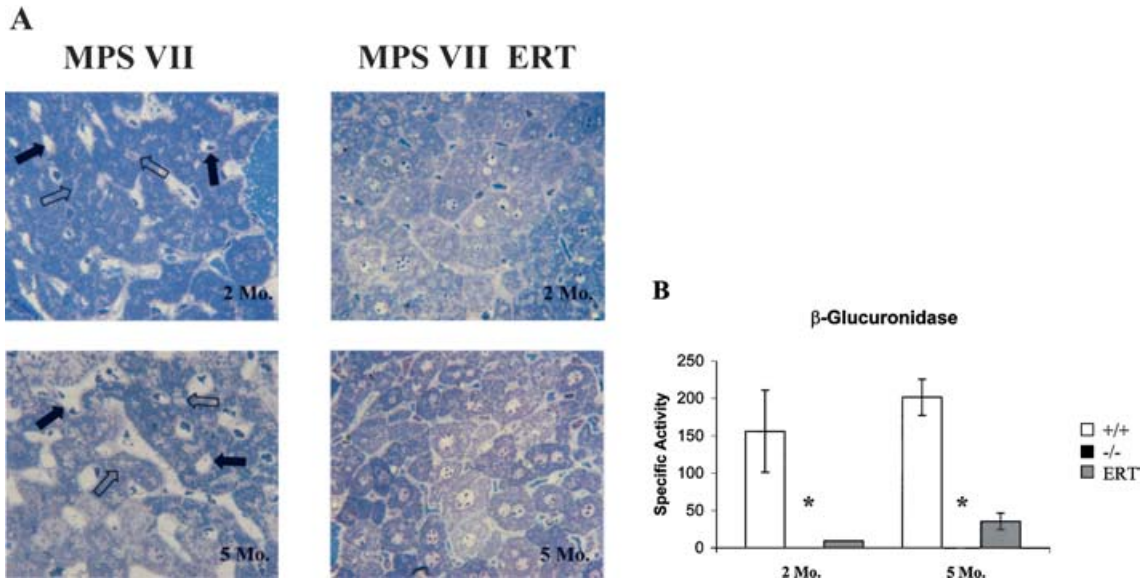

Figure 1 Decrease in lysosomal storage material in the liver at both the 2- and 5-month time points after ERT

(**A**) Distended lysosomes are seen in Kupffer cells (filled arrows) and hepatocytes (open arrows) of untreated MPS VII. Lysosomal storage is dramatically decreased in the animals that received ERT (MPS VII ERT). Magnification, 330×. (**B**) GUSB-specific activity (nmol of substrate cleaved/h per mg of protein) was measured in untreated normal (+/+; open bars), untreated MPS VII (−/−; black bars), and enzyme-replaced MPS VII (ERT; grey bars) animals. The values represent an average of three animals from each group, and the error bars represent ±1 S.D. *, GUSB levels that were less than 0.1 unit.

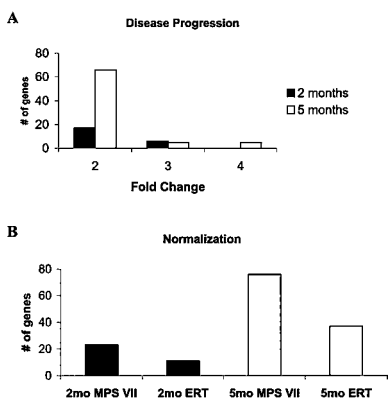

Figure 2 Increase in the number of genes with altered expression, and the percentage that return to baseline as the disease progresses

(**A**) The number of genes that have 2-, 3- and 4-fold changes are shown at 2 and 5 months of age. (**B**) shows that 52 % of the genes with altered expression at 2 months of age (2mo MPS VII) return to baseline following enzyme replacement (2mo ERT); 51 % of the genes with altered expression at 5 months of age (5mo MPS VII) returned to baseline following enzyme replacement (5mo ERT). Both up-regulated and down-regulated genes are included in this analysis.

higher in the 5moERT animals when compared with the 2moERT animals. Importantly, at both time points, approx. 50 % of the genes did not completely respond to therapy, or were resistant to therapy.

Confirmation of microarray results by real-time RT-PCR

Quantitative RT-PCR was used as an independent method to confirm the gene expression changes of a selected set of genes identified using the microarray technology. We selected both lysosome-associated and non-lysosomal genes for confirmation analysis. The trend (increased or decreased) of the expression changes detected by microarray analysis was confirmed by quantitative RT-PCR (Table 1, 'Non-lysosome associated genes' group). However, the magnitudes of the changes obtained by quantitative RT-PCR were greater than those obtained by GeneChip for Cyp4a14, IGFBP2 (insulin-like-growth-factor-binding protein 2), metallothionein 1 and SAA-2 (serum amyloid A gene-2).

Alterations in lysosomal proteins

Within cells that have established lysosomal storage, the size and number of lysosomes increase over time. Because of this increase, one might predict that, on average, there would be more lysosomal proteins per cell in the disease state. Therefore we compared changes in the mRNA levels and activities of several lysosomal enzymes in liver tissue. The activities of β-hexosaminidase, α-galactosidase and α-*N*-acetylglucosaminidase were elevated in MPS VII mice at both 2 months (6.5-, 3.5- and 3.6-fold respectively) and 5 months of age (Figures 3A–3D). In contrast, acid sphingomyelinase activity was decreased 1.3-fold at 2 months of age.

When we measured mRNA levels of the four lysosomal enzymes mentioned above by microarray analysis, three out of four of them were undetected at 2 months of age, and the fourth (acid sphingomyelinase) had a small, but less than 2-fold, change (Table 1). Using the more sensitive quantitative RT-PCR technique, we observed a small increase in the mRNA for β-hexosaminidase (2.62 ± 1.07-fold), α-galactosidase (2.06 ± 0.38-fold), α-*N*-acetylglucosaminidase (1.39 ± 0.22-fold), and acid sphingomyelinase (1.52 ± 0.25-fold) at 2 months of age compared with wild-type levels (Table 1). In the group of lysosome-associated genes that were detectable and had a change in expression by microarray analysis, a trend for subtle (less-than-2-fold) increases in message that was more pronounced at 5 months of age than at 2 months of age was observed. These increases at 5 months of age tended to be reduced by therapy (Table 2).

Table 1 Quantitative RT-PCR analysis on selected genes

Selected genes whose expression was changed 2-fold or greater (Non-lysosome-associated genes) at 2 months in the livers of MPS VII mice compared with wild-type mice were independently tested by quantitative RT-PCR. Lysosome-associated genes were also analysed by quantitative RT-PCR. Values reported (means ± S.D.) are fold increases (↑) or decreases (↓) in comparison with wild-type mRNA levels. Asterisks indicate mRNA species which were undetected by microarray analysis in wild-type liver at 2 months. det., mRNA was detected in the experimental group (MPS VII or MPS VII ERT) but undetectable in the wild-type group at that time point; NC, no change in expression levels compared with wild-type (the numbers following in parentheses show actual data from quantitative RT-PCR analysis); n.d., mRNA was not detected. CD-MPR, cation-dependent MPR; Cyp4a14 is a novel murine P450 gene; GalA, α-galactosidase; HexB, β-hexosaminidase; Naglu, α-*N*-acetylglucosaminidase; SAA-2, serum amyloid A gene-2; Smpd1, acid sphingomyelinase; VCAM-1, vascular cell adhesion molecule-1.

	GeneChip		Quantitative RT-PCR	
Gene	MPS VII	MPS VII ERT	MPS VII	MPS VII ERT
Non-lysosome-associated genes				
Cyp4a14	↑3.2	↑3.0	↑7.92 ± 0.39	↑6.68 ± 0.64
IGFBP2	↑2.5	↑2.5	↑4.70 ± 0.93	↑5.38 ± 1.08
Metallothionein 1	↑3.5	↑3.7	↑9.63 ± 1.30	↑7.40 ± 3.01
Chp-pending (P22)	↑2.3	↑2.8	NC(1.11 ± 0.09)	↑1.41 ± 0.26
SAA-2	↓3.5	↓7.5	↓6.33 ± 1.30	↓21.26 ± 2.16
VCAM-1*	det.	det.	↑2.12 ± 0.23	NC(0.83 ± 0.19)
Lysosome-associated genes				
Mannose receptor	NC	n.d.	↓1.85 ± 0.15	↓1.67 ± 0.27
CI-MPR	n.d.	n.d.	↓1.56 ± 0.32	
CD-MPR	NC	NC	NC(0.94 ± 0.13)	NC(1.14 ± 0.25)
LAMP1	NC	NC	NC(0.92 ± 0.16)	NC(1.09 ± 0.13)
Smpd1	↑1.3	NC	↑1.53 ± 0.25	↑1.23 ± 0.12
GalA*	n.d.	n.d.	↑2.05 ± 0.38	
HexB*	n.d.	n.d.	↑2.63 ± 1.08	
Naglu*	n.d.	det.	↑1.39 ± 0.22	

An increase in LAMP-1 was also observed in the MPS VII mice. A Western blot of liver homogenate from 2-month-old MPS VII mice probed with an anti-LAMP-1 antibody detected an approx. 3-fold increase in LAMP-1 protein (Figure 4A). In contrast with the transcriptional changes observed with lysosomal hydrolases, LAMP-1 mRNA was not increased in the MPS VII livers at either 2 months (Table 2) or 5 months (results not shown) of age. However, at 5 months of age, the mRNA for an alternatively spliced variant of LAMP2, LAMP2b [28], was increased 2.3-fold in the MPS VII mice (see the Supplemental Table at http://www.BiochemJ.org/bj/379/bj3790461add.htm). Interestingly, LAMP-2a expression was not changed.

We hypothesized that there may be changes in the levels of proteins involved in lysosome trafficking, in addition to the changes in the levels of various proteins in the mature lysosome. Microarray analysis did not detect any change in the mRNA levels of the mannose receptor (Table 1). In contrast, the mRNA for the CI-MPR was not detected by microarray in MPS VII mice. A small decrease in mannose-receptor mRNA (1.84 ± 0.14-fold) and CI-MPR mRNA (1.56 ± 0.32-fold) was detected by quantitative RT-PCR in MPS VII liver tissue. Western blots of both receptors showed little change in protein in the MPS VII disease state (Figures 4B and 4C). The mRNA levels of the cation-dependent MPR were unchanged by either microarray or quantitative RT-PCR (Table 1). Genes implicated in the transportation of cargo from the TGN (*trans*-Golgi network) to the late endosome and finally to the mature lysosome were also analysed for transcriptional changes at the 5-month time point. The AP (adaptor protein)-1 or the AP-3 complex components [29] that were detected on the GeneChip showed no transcriptional changes. Neither Rab7 mRNA (with Rab7 being implicated in transport to the lysosome [30]) nor Rab9 mRNA (with Rab9 being required for MPR recycling from the late endosome to the TGN [31]) were changed in the disease state. In addition, syntaxin 7 and VAMP-7 (vesicle-associated membrane protein 7), which are involved in lysosome fusion [32], were unchanged (results not shown).

Altered gene expression occurs in multiple metabolic pathways

The morphology of Kupffer cells in an MPS VII liver is grossly distorted (Figure 1A). Hepatocytes accumulate less storage and maintain their overall morphology. However, hepatocytes as well as Kupffer cells may be adapting to the gross morphological changes observed in the Kupffer cells. Several cell-adhesion genes, such as those for Ly-6A/E, N-cadherin and VCAM1 (vascular cell adhesion molecule 1), were up-regulated at various ages. At 5 months of age, Myo1b, Cappa2 (capping protein α2) and CDC10/Septin7, all of which interact with the cytoskeleton, were also up-regulated (Table 3) [33–35].

The growth hormone/IGF axis may also be disrupted in the MPS VII mice. Both IGFBP1 and IGFBP2 were increased at both 2 and 5 months of age. Additionally, at 5 months of age, expression of the growth-hormone receptor was increased (Table 3).

The original report of the MPS VII mouse as the adipose-storage-deficiency mouse directed our attention towards genes involved in lipid metabolism [10]. At 5 months of age, genes involved in the production of fatty acids, such as those for pyruvate kinase, fatty acid synthase, acyl-CoA synthase 4 and Δ^5-desaturase, had increases in expression (Table 3). Acyl-CoA synthase 4 specifically utilizes arachidonic acid, and studies of this protein suggest that the acyl-CoA that it produces is fated for triacylglycerol or phospholipid synthesis [36]. Additionally, Δ^5-desaturase desaturates eicosatrienoic acid (20:3$n-6$) to arachidonic acid (20:4$n-6$). No statistically significant difference was found in the plasma levels of NEFAs (non-esterified fatty acids) [0.62 ± 0.17 mM for homozygous MPS VII mice ($n = 13$) compared with 0.56 ± 0.13 mM for wild-type/heterozygous mice ($n = 20$)] or triacylglycerols [54 ± 11 mg/dl for homozygous MPS VII mice ($n = 13$) compared with 60 ± 15 mg/dl for wild-type/heterozygous mice ($n = 20$)] between MPS VII mice and homozygous and heterozygous control mice at 5 months of age.

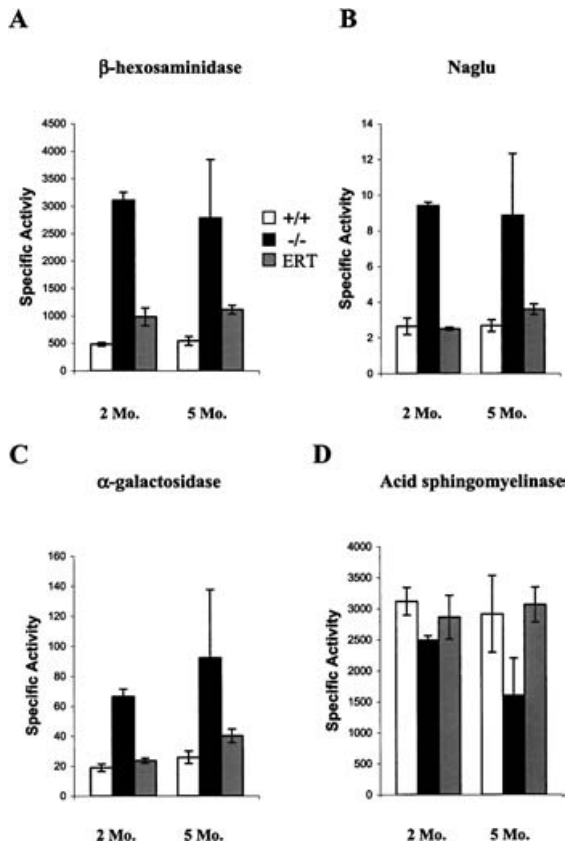

Figure 3 Secondary changes in liver lysosomal enzyme activities after ERT

The specific activities (nmol of substrate cleaved/h per mg of protein) of β-hexosaminidase (**A**), *N*-acetylglucosaminidase (**B**; Naglu), α-galactosidase (**C**) and acid sphingomyelinase (**D**; arbitrary fluorescence units/h per mg of protein) in untreated normal (+/+), untreated MPS VII (−/−) and enzyme-replaced MPS VII (ERT) animals are shown at 2 and 5 months. Each group represents the average of three animals, and the error bars represent ± 1 S.D. Interestingly, the magnitude of the changes in enzyme activities is not equivalent to the changes in expression (see Table 1).

Table 2 Lysosome-associated genes with altered expression in MPS VII mice compared with wild-type mice

Values reported are fold increases (↑) or decreases (↓) in comparison with wild-type mRNA levels. NC, no change in expression levels compared with wild-type.

		MPS VII	MPS VII ERT	MPS VII	MPS VII ERT
Gene name	Age (months) . . .	2		5	
Arylsulphatase A		NC	NC	↑1.6	NC
Cathepsin A		↑1.4	↑1.3	↑1.9	↑1.4
Cathepsin Z		NC	↑1.4	↑1.7	↑1.9
Cln2		NC	NC	↑1.9	↑1.5
Hexosaminidase A		NC	↑1.2	↑1.4	NC
Cathepsin B		NC	NC	↑1.5	NC
Npc1		NC	NC	↑1.6	NC
Cathepsin S		NC	↓1.6	↑1.4	NC

The second pathway that emerged is involved in the biogenesis and cellular efflux of cholesterol. Genes involved in virtually the entire cholesterol-synthesis pathway had an increased expression at 5 months of age. SREBP1 (sterol-regulatory-element-binding protein 1) mRNA was also induced by an appreciable degree (1.5-fold over wild-type). The genes for ABCA1 (ATP-binding cassette transporter A1) and ApoA-IV (apolipoprotein A-IV),

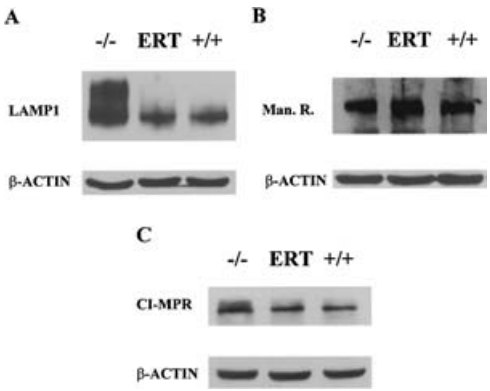

Figure 4 GUSB deficiency leading to changes in certain membrane-bound lysosomal proteins

Western blot analysis was performed on liver homogenates from 2-month-old normal (+/+), MPS VII (−/−) and enzyme-replaced MPS VII (ERT) mice. The blots were probed with antibodies directed against LAMP-1 (**A**), the mannose receptor (Man. R.) (**B**), and the CI-MPR (**C**). Equal amounts of protein were loaded in each lane, and the blots were probed with an anti-β-actin antibody as a loading control.

which are implicated in reverse cholesterol transport, had elevated expression at the 5-month time point (Table 4) [37,38]. In agreement with results published previously [10], plasma cholesterol was significantly reduced in the MPS VII mice compared with homozygous and heterozygous controls at 5 months of age [61 ± 18 mg/dl for MPS VII homozygous mice ($n = 13$) compared with 105 ± 17 mg/dl for wild-type/heterozygous mice ($n = 20$); $P < 0.0001$]. Importantly, a group of 4.5-month-old MPS VII mice that were given ERT according to the regimen described in the Experimental section, and which resulted in an average of 15.6 ± 3.9 % of the mean wild-type levels of GUSB, had cholesterol levels that were not normalized by the therapy [56 ± 6 mg/dl for ERT-treated MPS VII mice ($n = 3$); $P < 0.65$]. Notably, the increases in mRNA for genes of the cholesterol-biosynthesis pathway in MPS VII mice were only partially normalized by ERT (Table 4). Interestingly, we also found significantly less plasma cholesterol ($P < 0.01$) in 3-month-old MPS VII mice ($n = 4$) compared with homozygous and heterozygous controls ($n = 10$; results not shown).

DISCUSSION

ERT is becoming the therapy of choice for several LSDs. A better understanding of the molecular consequences of this approach will lead to further improvements. In order to identify additional molecular targets that may increase the efficacy of ERT, we determined the biochemical and molecular effects of both GUSB deficiency and ERT. Although the progressive accumulation of partially degraded GAGs affects multiple organ systems in the MPS VII mouse, we chose to study the liver for several reasons. First, the liver is severely affected by this disease. Both hepatocytes and Kupffer cells accumulate storage material and have lysosomal distention that is easily visible by light microscopy. Secondly, the liver responds well to various therapies. In particular, the lysosomal distention present in both hepatocytes and Kupffer cells can be virtually eliminated by ERT in as little as 48 h [20]. Thirdly, the relatively small number of cell types in the liver would allow for easier interpretation of microarray results. The liver is composed primarily of two cell types: hepatocytes (80–85 %) and Kupffer cells (15–20 %). Finally, the liver directly interacts with multiple organ systems. Therefore we thought that

Table 3 Secondary alterations in non-lysosome-associated genes in MPS VII mice

Selected genes with altered expression at 2 or 5 months of age in MPS VII mice compared with wild-type mice. Values reported are fold increases, ↑, or decreases, ↓, in comparison with wild-type mRNA levels. NC, no change in expression levels compared with wild-type; det., mRNA was detected in the experimental group (MPS VII or MPS VII ERT), but was undetectable in the wild-type group at that time point. ACS4, acyl-CoA synthase 4; Cappa2, capping protein $\alpha 2$; D5D, Δ^5-desaturase; FASN, fatty acid synthase; Ghr, growth-hormone receptor; Pklr, pyruvate kinase; VCAM-1, vascular cell adhesion molecule-1

		MPS VII	MPS VII ERT	MPS VII	MPS VII ERT
Accession no./gene name	Age (months) . . .	2		5	
Cell adhesion					
Ly-6A/E		↑2.3	NC	↑1.6	NC
Cdh2/N-cadherin		NC	NC	↑2.0	↑3.2
VCAM-1		det.	det.	↑3.2	↑3.2
Cytoskeleton					
Myosin I/Myo1b		NC	NC	↑2.0	↑1.7
Cappa2		NC	NC	↑2.3	NC
CDC10/Septin7		NC	NC	↑2.5	↑2.6
Growth hormone/IGF axis					
IGFBP1		↑2.0	↓1.9	↑1.7	↑3.0
IGFBP2		↑2.5	↑2.5	↑1.5	↑2.1
Ghr		↑1.7	NC	↑2.5	NC
Lipid metabolism					
Pklr		↓1.4	NC	↑2.1	NC
FASN		NC	NC	↑1.5	↑1.3
AA619207/ACS4		NC	NC	↑2.0	↑3.5
AI853364/D5D		NC	NC	↑2.1	↑1.7

Table 4 Increased expression of cholesterol-metabolism genes in untreated and ERT-treated MPS VII mice at the age of 5 months

Values reported are fold increases (↑) in comparison with wild-type mRNA levels. NC, no change in expression levels compared with wild-type. ABCA1, ATP-binding cassette transporter A1; ApoA-IV, apolipoprotein A-IV; HMG-CoA synthase, 3-hydroxy-3-methylglutaryl-CoA synthase; SREBP1, sterol-regulatory-element-binding protein 1.

	Mouse	
Gene	MPS VII	MPS VII ERT
Cholesterol metabolic genes		
SREBP1	↑1.5	NC
AW124932/HMG-CoA synthase	↑2.0	NC
AA716963/isopentenyl pyrophosphate isomerase	↑4.3	↑3.5
Farnesyl diphosphate synthase	↑4.0	↑2.0
Sterol-C5-desaturase	↑2.6	NC
AW106745/Nsdhl	↑2.0	NC
AI848668/Sterol-C4-methyloxidase-like	↑2.8	↑3.5
Reverse cholesterol transport		
AI845514/ABCA1	↑2.0	↑2.5
ApoA-IV	↑2.5	NC

the liver might provide insights into primary and secondary adaptations to LSD on both an organ and organismal level.

LSDs are progressive metabolic disorders in which the clinical presentation becomes increasingly severe and complex. MPS VII is no exception. Altered gene expression was more evident at 5 months of age than at 2 months of age. Notably, after ERT at either time point, numerous transcriptional alterations persisted. It is possible that with higher doses of enzyme or longer treatment regimens more of these changes would have been normalized. Although the reduction in lysosomal distention is virtually identical regardless of whether the therapy is initiated early in life or later, the clinical outcome is different [13,20]. In addition, although therapy initiated early in life, rather than later, results in a more complete clinical response, some pathologies persist. These observations suggest that there are disease-related changes, that cannot be studied by conventional clinical assays. Moreover these observations also suggest that there are clinical defects that are caused by secondary alterations that may be completely unrelated to the levels of accumulating intralysosomal GAGs. This is highlighted by the fact that numerous transcriptional changes persist at both 2 and 5 months, even after histological evidence of lysosomal storage is absent. The results reported here identify a set of molecular markers that probably contribute to the secondary disease phenotype and, therefore, are potential targets for improving existing therapies.

One property of many LSDs is the secondary elevation of both lysosomal membrane proteins and other lysosomal enzyme activities [8]. Often, the alterations of these proteins are only partially normalized by ERT. The mechanisms behind the expansion of lysosomes and their constituents are poorly understood. A series of studies have identified transcriptional alterations that may account for some of these changes. Brooks et al. [39] observed a reduction in mRNA levels (>2-fold) of two lysosomal enzymes in the brains of MPS VII mice in response to gene therapy. In contrast, Potratz et al. [40] saw no increase in mRNAs for several lysosomal hydrolases in mouse models of GM2 gangliosidoses and prosaposin deficiency. The differences in the studies cited above may reflect variability between cellular responses to the accumulation of lipids compared with GAGs. However, it remained unclear whether the changes in transcription accounted completely for the changes in protein or activity levels. The data presented here strongly suggest that both transcriptional and post-transcriptional mechanisms are involved in the increases in enzyme activity, since the magnitude of the increased expression (1–2-fold) is less than the increase in activity (3–6-fold). Conversely, the increase in LAMP-1 appears to be regulated primarily by post-transcriptional mechanisms.

The decrease in acid sphingomyelinase activity in MPS VII liver tissue at 2 months of age and the larger reduction at 5 months may be due to inhibition by GAGs, as has been observed with other lysosomal enzymes [41,42]. This decrease is significant, since the sphingomyelin content in cells can affect the rate of cholesterol synthesis. It has been shown previously that, when sphingomyelin was added to cells, cholesterol synthesis was increased [43]. This

could contribute to the increase in expression of genes involved in cholesterol biosynthesis observed in this study. Enzyme replacement, while normalizing sphingomyelinase activity, only partially corrected the changes in cholesterol biosynthesis genes.

Interestingly, the machinery necessary for the transport of intracellular and extracellular lysosomal proteins appears to be intact. For instance, there were no large increases in the protein levels of the mannose receptor or the CI-MPR. This finding is significant, since it was previously unknown how GAG accumulation affected these receptors, and both receptors are involved in the uptake of recombinant enzyme during ERT [19]. In addition, there were no transcriptional increases in the mRNAs for several other proteins involved in transport from the TGN to the lysosome or in the endosomal system. This suggests that wild-type levels of these proteins can keep pace with the expansion of lysosomes in the diseased state.

A common finding in patients with MPS is short stature. MPS VII mice are noticeably smaller than their wild-type littermates. The mice have osteoclast defects that contribute to their bone disease and smaller size [44]. However, it is also possible that an altered growth hormone/IGF axis affects the bone growth and overall mass of MPS VII animals. In support of this hypothesis, the expression of the genes for IGFBP1 and IGFBP2 was upregulated in MPS VII mice at both time points. IGFBPs regulate the available amount of free IGFs in the serum. Interestingly, transgenic mice that overexpress IGFBP1 or IGFBP2 have reduced body size [45].

Both the biochemical and transcription data in the current study suggest that GUSB deficiency may induce physiological malnutrition in the MPS VII mice, which leads to the profound adipose storage deficiency. An animal model that may provide insights into the adipose storage deficiency observed in MPS VII is the chylomicron-deficient mouse. The chylomicron-deficient mouse represents an animal model of fat malabsorption [46,47]. These mice have normal levels of circulating NEFAs [47] and triacylglycerols, yet lower levels of high-density lipoprotein/cholesterol [46]. In addition, these mice have very low adiposity. Also, lipogenesis, cholesterogenesis and triacylglycerol synthesis are all increased in the liver. The MPS VII mouse has many of these same molecular changes, in addition to the adipose storage deficiency.

In the original description of the GUSB-deficient mouse that noted the adipose storage deficiency, the storage of fatty acids only occurred in the form of liver triacylglycerols [10]. It was also reported that the mice had lower levels of cholesterol, in agreement with the results reported in the present study. Consistent with the observations in chylomicron-deficient mice, we observed normal levels of NEFA and triacylglycerols, as well as increased expression of genes involved in lipogenesis, cholesterogenesis and triacylglycerol synthesis. The induction of lipoprotein lipase expression, a gene not normally expressed in the adult mammalian liver, at 5 months of age in MPS VII mice compared with wild-type mice (MPS VII P value for detection of < 0.04, 7-fold higher signal than the background signal of wild-type) suggests that the liver is in greater need of NEFAs than normal (results not shown). This is consistent with the increased expression of lipid and triacylglycerol synthesis genes.

The alterations in the expression of lipid metabolism genes, consistent with malnutrition, and the adipose storage deficiency may all be specific to the MPS VII mouse. However, some of the metabolic changes observed in MPS VII mice may be common to other LSDs in mouse and human. For example, we also see an adipose storage deficiency in mouse models of MPS type I and Niemann-Pick type A/B (J. Woloszynek and M. S. Sands, unpublished work). In addition, it is possible that the proposed malnutrition could be the result of reduced ingestion of nutrients or malabsorption. Malabsorption of dietary fats in humans can result in episodes of diarrhoea. There are anecdotal reports that patients with MPS II and MPS III can suffer from chronic, sometimes severe, diarrhoea [4].

This study represents a comprehensive identification of global transcriptional changes in the livers of MPS VII and enzyme-replaced MPS VII mice in comparison with wild-type mice. The changes in transcription that are not normalized by ERT represent additional therapeutic targets which could increase the efficacy of this approach. In addition, both transcriptional and post-transcriptional mechanisms account for the primary lysosomal defects observed in MPS VII mice. Also, alterations in several seemingly unrelated pathways could account for the complex phenotype of these animals. Finally, this data set will serve as a resource for future experiments designed to understand further the pathology of other MPSs and LSDs, and to improve the efficacy of existing therapies.

We thank Dr Philip Stahl and Dr Stuart Kornfeld for generously giving the anti-(mannose receptor) antibody and anti-MPR antibody respectively. This work was supported in part by National Institutes of Health grants DK57586 (M. S. S.), GM 34182 (W. S.), HL58427 (C. F. S.), DK56341 (C. F. S.), DK 20579 (C. F. S.) and a grant from the Siteman Cancer Center at Washington University.

REFERENCES

1 Mullins, C. and Bonifacino, J. (2001) The molecular machinery for lysosome biogenesis. BioEssays **23**, 333–343
2 Neufeld, E. (1991) Lysosomal storage diseases. Annu. Rev. Biochem. **60**, 257–280
3 Sly, W., Quinton, B., McAlister, W. and Rimoin, D. (1973) β-glucuronidase deficiency: report of clinical, radiologic and biochemical features of a new mucopolysaccharidosis. J. Pediatr. **82**, 249–257
4 Neufeld, E. and Muenzer, J. (2001) The mucopolysaccharidoses. In The Metabolic and Molecular Bases of Inherited Disease (Scriver, C., Beaudet, A., Sly, W., Valle, D., Vogelstein, B. and Childs, B., eds.), pp. 3421–3452, McGraw-Hill, New York
5 Birkenmeier, E., Davisson, M., Beaver, W., Ganschow, R., Vogler, C., Gwynn, B., Lyford, K., Maltais, L. and Wawrzyniak, C. (1989) Murine mucopolysaccharidosis type VII. Characterization of a mouse with β-glucuronidase deficiency. J. Clin. Invest. **83**, 1258–1266
6 Vogler, C., Birkenmeier, E., Sly, W., Levy, B., Pegors, C., Kyle, J. and Beamer, W. (1990) A murine model of mucopolysaccharidosis VII. Gross and microscopic findings in β-GUSB-deficient mice. Am. J. Pathol. **136**, 207–217
7 Sands, M. and Birkenmeier, E. (1993) A single-base-pair deletion in the β-glucuronidase gene accounts for the phenotype of murine mucopolysaccharidosis type VII. Proc. Natl. Acad. Sci. U.S.A. **90**, 6567–6571
8 Birkenmeier, E., Barker, J., Vogler, C., Kyle, J., Sly, W., Gwynn, B., Levy, B. and Pegors, C. (1991) Increased life span and correction of metabolic defects in murine mucopolysaccharidosis type VII after syngeneic bone marrow transplantation. Blood **78**, 3081–3092
9 Frisella, W., O'Conner, L., Vogler, C., Roberts, M., Walkley, S., Levy, B., Daly, T. and Sands, M. (2001) Intracranial injection of recombinant adeno-associated virus improves cognitive function in a murine model of mucopolysaccharidosis type VII. Mol. Ther. **3**, 351–358
10 Beamer, W. and Coleman, D. (1982) Mouse Newsletter **67**, 21
11 Casal, M. and Wolfe, J. (1998) Variant clinical course of mucopolysaccharidosis type VII in two groups of mice carrying the same mutation. Lab. Invest. **78**, 1575–1581
12 Vogler, C., Barker, J., Sands, M., Levy, B., Galvin, N. and Sly, W. (2001) Murine mucopolysaccharidosis VII: impact of therapies on the phenotype, clinical course, and pathology in a model of a lysosomal storage disease. Pediatr. Dev. Pathol. **4**, 421–433
13 Sands, M., Vogler, C., Torrey, A., Levy, B., Gwynn, B., Grubb, J., Sly, W. and Birkenmeier, E. (1997) Murine mucopolysaccharidosis type VII: long term therapeutic effects of enzyme replacement and enzyme replacement followed by bone marrow transplantation. J. Clin. Invest. **99**, 1596–1605
14 Sands, M., Barker, J., Vogler, C., Levy, B., Gwynn, B., Galvin, N., Sly, W. and Birkenmeier, E. (1993) Treatment of murine mucopolysaccharidosis type VII by syngeneic bone marrow transplantation in neonates. Lab. Invest. **68**, 676–686
15 Daly, T., Ohlemiller, K., Roberts, M., Vogler, C. and Sands M. (2001) Prevention of systemic clinical disease in MPS VII mice following AAV-mediated neonatal gene transfer. Gene Ther. **8**, 1291–1298

16 Sands, M., Erway, L., Vogler, C., Sly, W. and Birkenmeier, E. (1995) Syngeneic bone marrow transplantation reduces the hearing loss associated with murine mucopolysaccharidosis type VII. Blood **86**, 2033–2040
17 Ohlemiller, K., Vogler, C., Roberts, M., Galvin, N. and Sands, M. (2000) Retinal function is improved in a murine model of a lysosomal storage disease following bone marrow transplantation. Exp. Eye Res. **71**, 469–481
18 Wolfe, J. and Sands, M. (1996) Murine mucopolysaccharidosis type VII: a model system for somatic gene therapy of the central nervous system. In Gene Therapy into Neurones, Towards Gene Therapy of Neurological Disorders (Lowenstein, P. and Enquist, L., eds.), pp. 263–274, John Wiley and Sons, Chichester
19 Sands, M., Vogler, C., Ohlemiller, K., Roberts, M., Grubb, J., Levy, B. and Sly, W. (2001) Biodistribution, kinetics, and efficacy of highly phosphorylated and non-phosphorylated β-glucuronidase in the murine model of mucopolysaccharidosis VII. J. Biol. Chem. **276**, 43160–43165
20 Sands, M., Vogler, C., Kyle, J., Grubb, J., Levy, B., Galvin, N., Sly, W. and Birkenmeier, E. (1994) Enzyme replacement therapy for murine mucopolysaccharidosis type VII. J. Clin. Invest. **93**, 2324–2331
21 He, X., Chen, F., McGovern, M. and Schuchman, E. (2002) A fluorescence-based, high-throughput sphingomyelin assay for the analysis of Niemann-Pick disease and other disorders of sphingomyelin metabolism. Anal. Biochem. **306**, 115–123
22 Tordjman, K., Bernal-Mizrachi, C., Zemany, L., Weng, S., Feng, C., Zhang, F., Leone, T., Coleman, T., Kelly, D. and Semenkovich, C. (2001) PPARα deficiency reduces insulin resistance and atherosclerosis in apoE-null mice. J. Clin. Invest. **107**, 1025–1034
23 Casal, M. and Wolfe, J. (2000) Mucopolysaccharidosis type VII in the developing mouse fetus. Pediatr. Res. **47**, 750–756
24 Vogler, C., Sands, M., Higgins, A., Levy, B., Grubb, J., Birkenmeier, E. and Sly, W. (1993) Enzyme replacement with recombinant β-glucuronidase in the newborn mucopolysaccharidosis type VII mouse. Pediatr. Res. **34**, 837–840
25 Wolfe, J., Deshmane, S. and Fraser, N. (1992) Herpesvirus vector gene transfer and expression of β-glucuronidase in the central nervous system of MPS VII mice. Nat. Genet. **1**, 379–384
26 Daly, T., Okuyama, T., Vogler, C., Haskins, M., Muzyczka, N. and Sands, M. (1999) Neonatal intramuscular injection with recombinant adeno-associated virus results in prolonged β-glucuronidase expression in situ and correction of liver pathology in mucopolysaccharidosis type VII mice. Hum. Gene Ther. **10**, 85–94
27 Vogler, C., Sands, M., Levy, B., Galvin, N., Birkenmeier, E. and Sly, W. (1996) Enzyme replacement with recombinant β-glucuronidase in murine mucopolysaccharidosis type VII: impact of therapy during the first six weeks of life on subsequent lysosomal storage, growth, and survival. Pediatr. Res. **39**, 1050–1054
28 Konecki, D., Foetisch, K., Zimmer, K., Schlotter, M. and Lichter-Konecki, U. (1995) An alternatively spliced form of the human lysosome-associated membrane protein-2 gene is expressed in a tissue-specific manner. Biochem. Biophys. Res. Commun. **215**, 757–767
29 Reusch, U., Bernhard, O., Koszinowski, U. and Schu, P. (2002) AP-1A and AP-3A lysosomal sorting functions. Traffic **3**, 752–761
30 Press, B., Feng, Y., Hoflack, B. and Wandinger-Ness, A. (1998) Mutant Rab7 causes the accumulation of cathepsin D and cation-independent mannose 6-phosphate receptor in an early endocytic compartment. J. Cell Biol. **140**, 1075–1089
31 Riederer, M., Soldati, T., Shapiro, A., Lin, J. and Pfeffer, S. (1994) Lysosome biogenesis requires Rab9 function and receptor recycling from endosomes to the *trans*-Golgi network. J. Cell Biol. **125**, 573–582
32 Ward, D., Pevsner, J., Scullion, M., Vaughn, M. and Kaplan, J. (2000) Syntaxin 7 and VAMP-7 are soluble *N*-ethylmaleimide-sensitive factor attachment protein receptors required for late endosome–lysosome and homotypic lysosome fusion in alveolar macrophages. Mol. Biol. Cell **11**, 2327–2333
33 Tang, N. and Ostap, E. (2001) Motor domain-dependent localization of myo1b (myr-1). Curr. Biol. **11**, 1131–1135
34 Hart, M., Korshunova, Y. and Cooper, J. (1997) Vertebrates have conserved capping protein α isoforms with specific expression patterns. Cell Motil. Cytoskeleton **38**, 120–132
35 Field, C. and Kellogg, D. (1999) Septins: cytoskeletal polymers or signalling GTPases? Trends Cell Biol. **9**, 387–394
36 Coleman, R., Lewin, T., Van Horn, C. and Gonzalez-Baró, M. (2002) Do long-chain acyl-CoA synthetases regulate fatty acid entry into synthetic versus degradative pathways? J. Nutr. **132**, 2123–2126
37 Attie, A., Kastelein, J. and Hayden, M. (2001) Pivotal role of ABCA1 in reverse cholesterol transport influencing HDL levels and susceptibility to atherosclerosis. J. Lipid Res. **42**, 1717–1726
38 Fournier, N., Atger, V., Paul, J., Sturm, M., Duverger, N., Rothblat, G. and Moatti, N. (1999) Human ApoA-IV overexpression in transgenic mice induces cAMP-stimulated cholesterol efflux from J774 macrophages to whole serum. Arterioscler. Thromb. Vasc. Biol. **20**, 1283–1292
39 Brooks, A., Stein, C., Hughes, S., Heth, J., McCray, P., Sauter, S., Johnston, J., Cory-Slechta, D., Federoff, H. and Davidson, B. (2002) Functional correction of established central nervous system deficits in an animal model of lysosomal storage disease with feline immunodeficiency virus-based vectors. Proc. Natl. Acad. Sci. U.S.A. **99**, 6216–6221
40 Potratz, A., Hüttler, S., Bierfreund, U., Proia, R., Suzuki, K. and Sandhoff, K. (2000) Quantification of mRNAs encoding proteins of the glycosphingolipid catabolism in mouse models of GM2 gangliosidoses and sphingolipid activator protein precursor (prosaposin) deficiency. Biochim. Biophys. Acta **1502**, 391–397
41 Kint, J., Dacremont, G., Carton, D., Orye, E. and Hooft, C. (1973) Mucopolysaccharidosis: secondarily induced abnormal distribution of lysosomal isoenzymes. Science **181**, 352–354
42 Avila, J. and Convit, J. (1975) Inhibition of leucocytic lysosomal enzymes by glycosaminoglycans *in vitro*. Biochem. J. **152**, 57–64
43 Gatt, S. and Bierman, E. (1980) Sphingomyelin suppresses the binding and utilization of low density lipoproteins by skin fibroblasts. J. Biol. Chem. **255**, 3371–3376
44 Monroy, M., Ross, F., Teitelbaum, S. and Sands, M. (2002) Abnormal osteoclast morphology and bone remodeling in a murine model of a lysosomal storage disease. Bone **30**, 352–359
45 Schneider, M., Lahm, H., Wu, M., Hoeflich, A. and Wolf, E. (2000) Transgenic mouse models for studying the functions of insulin-like growth factor-binding proteins. FASEB J. **14**, 629–640
46 Young, S., Cham, C., Pitas, R., Burri, B., Connolly, A., Flynn, L., Pappu, A., Wong, J., Hamilton, R. and Farese, R. (1995) A genetic model for absent chylomicron formation: mice producing apolipoprotein B in the liver, but not in the intestine. J. Clin. Invest. **96**, 2932–2946
47 Jung, H., Turner, S., Neese, R., Young, S. and Hellerstein, M. (1999) Metabolic adaptations to dietary fat malabsorption in chylomicron-deficient mice. Biochem. J. **343**, 473–478

Received 11 July 2003/5 January 2004; accepted 6 January 2004
Published as BJ Immediate Publication 6 January 2004, DOI 10.1042/BJ20031048